High Resolution Silicon Accelerometer using Eutectic Bonding

Yun Kwang Jeon*, Soon Chang Yeon*, Yong Hyup Kim**, Seung Wu Rhee***, Shi Hwan Oh***

*: Research assistant, Seoul National University, Korea, aerojeon@aeroguy.snu.ac.kr
**: Corresponding author, Professor, Seoul National University, Korea
***: Korea Aerospace Research Institute, Korea

ABSTRACT

High precision micro-accelerometers are used in many applications such as automotives, aviations and aerospace navigation systems. In this paper, a lateral capacitive micro-accelerometer with μg level resolution has been designed and fabricated using simple micromachining process.

Large sensing area and large proof mass are important in the design of high precision accelerometer.[1-4] To satisfy these requirements, the differential capacitive comb type is adopted for the sensing part, and the bulk-micromachining is used to define the micro structure.

The height of the accelerometer is 50μm and in-plane dimension is 870μm × 1027μm. The sensing gap of 4μm is defined by Deep RIE process. Spring is 3~5μm thick and 200~300μm long. Proof mass weighs 15.84μg, and natural frequency of the accelerometer is 10.894kHz.

Keywords: Microaccelerometer, Differential capacitive, Bulk micromaching, Deep RIE.

1 INTRODUCTION

Numerous MEMS(Micro-Electro-Mechanical-System) acceleration sensors have been investigated.[1-9] There exist many types such as capacitive, piezoresistive, and piezoelectric. Among these types, differential capacitive MEMS accelerometer has many advantages such as high sensitivity, good linearity, low power consumption, low drift, and low fabrication cost.

Most of differential capacitive type in literature is fabricated by using surface micromaching which allows a few microns of structure height. Now, the evolution of fabrication technology enables making high aspect ratio structure using bulk-micromachining process and precision wafer bonding.

To make bulk micromachined differential capacitive type accelerometer, additional electrode layer is needed between substrate and structure. Although silicon on glass structure needs wafer bonding process, it is hard to make proper electrical connection and isolation between sensing elements. We resolved this electrical problem with eutectic bonding of glass wafer and silicon wafer.

2 ACCELEROMETER DESIGN

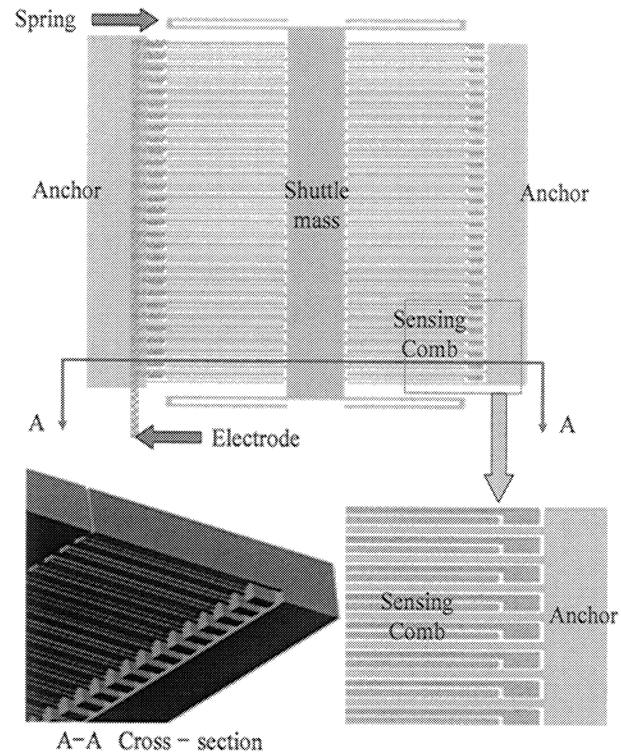

Figure 1 : Designed accelerometer

To achieve high resolution, an accelerometer should have maximum electrical sensitivity and minimum mechanical noise. Important design parameters which reduce noise and increase sensitivity, are large proof mass and large sensing area. Therefore, the noise equivalent acceleration due to Brownian motion of gas molecules should be considered[3,4] and expressed in Eqn. (1).

$$a_s = \frac{\sqrt{4KcT}}{9.8M} \quad (1)$$

where, K is Boltzmann constant, T is operating temperature, c is damping constants, and M is mass.

In Eqn. (1), mass and damping are function of structural geometry. So, the dimensions of the accelerometer is determined by optimization based on Eqn. (1).

2.1 Structure Design

Figure 1. shows the designed accelerometer layout. The physical model of an accelerometer can be expressed using mass-spring-damper system. Also the governing equation

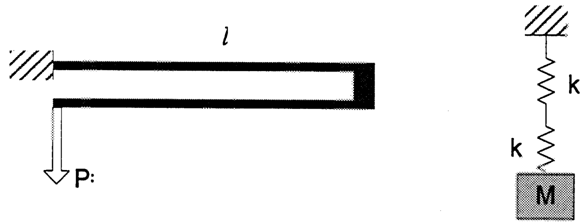

Figure 2 : Folded spring model

of this system can be written as Eqn. (2).

$$\ddot{x} + 2\varsigma\omega_n \dot{x} + \omega_n^2 x = a(t) \quad (2)$$

where, x is displacement of proof mass, natural frequency $\omega_n = (k/m)^{1/2}$, damping ratio $\varsigma = c/(2(mk)^{1/2})$, and $a(t)$ is input acceleration.

The proof mass of the system is composed of shuttle mass, spring and comb parts, and the total proof mass is expressed as follows :

$$m = \rho(A_{spring} + A_{shuttle} + A_{comb})H \quad (3)$$

where ρ is density of the silicon, and H is structure height.

Spring must be flexible to make large displacement when very small input force applied, and insensitive to cross-axis acceleration input. To satisfy this requirements, folded spring type is adopted in the present design as shown in Fig. 2, and stiffness of the spring expressed as follows :

$$k = 2 \cdot \frac{E \cdot H \cdot t^3}{l^3} \quad (4)$$

where, E is Yong's modulus, l is spring length, and t is spring thickness. The stiffness of the spring in the present design is 60.75N/m.

Damping constant which controls the frequency response of the sensor, must have the value larger than critical damping $(\varsigma > 2\sqrt{km})$ to avoid catastrophe of the sensor. Generally, Coutte flow, Stokes flow and Squeeze film effects are considered for damping in microstructure. Since Coutte and Stokes effect are much smaller than squeeze film damping effect. We considered only squeeze film damping effect in this study. The analytic solution of squeeze film damping coefficient for rectangular plate[10] can be expressed as follows :

$$c = 16 \cdot \mu \cdot f\left(\frac{L}{H}\right) \cdot H \cdot \left(\frac{L}{d}\right)^3 \quad (5)$$

where $f(L/H)$ is effect of aspect ratio on damping produced by a rectangular plate, μ is air damping constant, L is overlap length, and d is initial distance between two combs.

2.2 Sensing part

Figure 3 is schematic view of sensing part. When center proof mass is moving up and down, one side comb distance increases, while the other side decreases. It indicates that capacitance varies respectively.

The capacitance change can be expressed in Eqn. (6), and simplified as the expression in Eqn. (7). In Eqn. (7), the capacitance is linear in displacement of proof mass. Figure 4 shows results of capacitance with respect to the displacement based on Eqn. (6) and (7). Since the maximum displacement of proof mass is less than 1 μm, the linear assumption of capacitance in Eqn, (7) is proper for the present study.

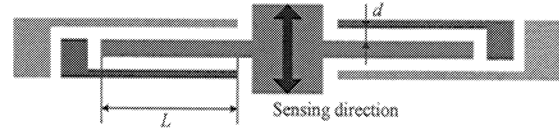

Figure 3 : Schematic view of sensing part.

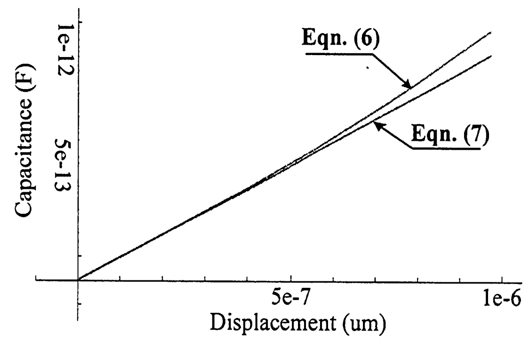

Figure 4 : Linearization

$$\Delta C = \varepsilon A\left(\frac{1}{d-x} - \frac{1}{d+x}\right) \quad (6)$$

$$\cong 2\varepsilon A \frac{x}{d^2} \quad (7)$$

The dimensions of the present accelerometer are summarized in table 1.

Design Variables	Calculated Value
Spring Length	220 ㎛ / 320 ㎛
Spring Thickness	3 ㎛ / 4 ㎛
Overlap Area	200 ㎛ X 50 ㎛
Number of Finger	60
Finger Thickness	4 ㎛
Air Gap	4 ㎛
Number of Spring	4

Table 1: Geometry parameters of the accelerometer

Using the designed 3D model, we simulated dynamic response analysis and FEM modal analysis and Figure 5 shows the results.

The analytic natural frequency calculated based on the mass and stiffness in Eqn. (3) and (4) is 10.575kHz. The detail numerical modeling of the accelerometer by using ANSYS yields the first natural frequency of 10.894kHz, which agrees well with the analytic natural frequency. In Fig. 5, the modes of 1st, 2nd, 3rd, 4th natural frequency computed by using ANSYS are plotted.

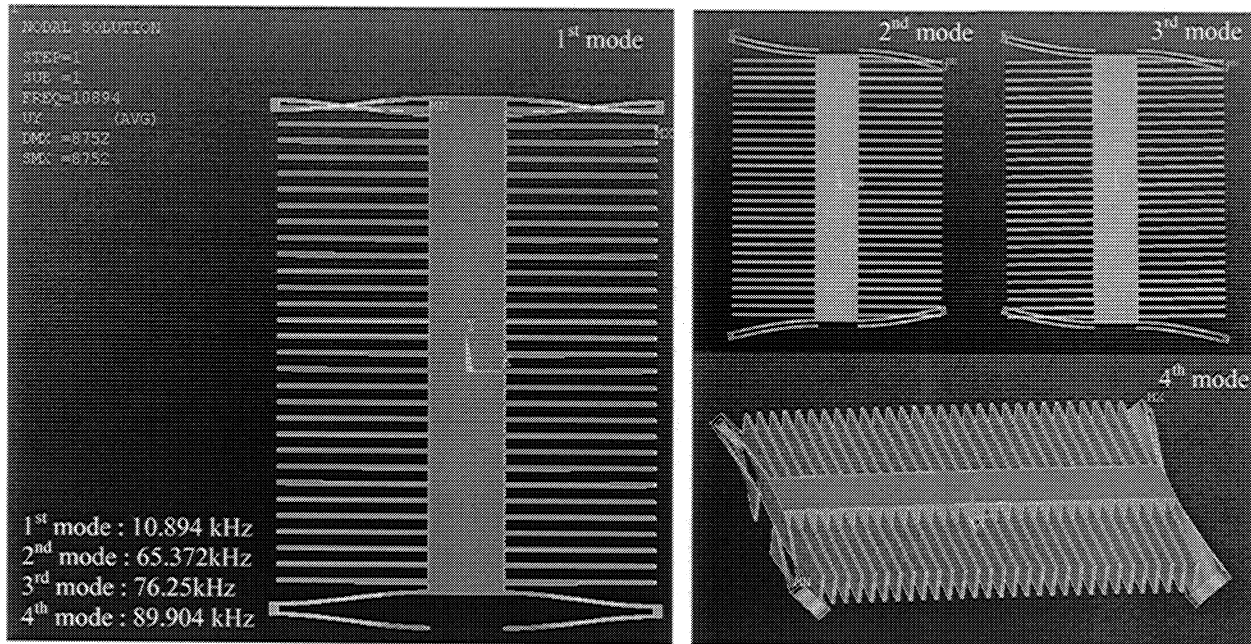

Figure 5 : Mode Analysis

3 FABRICATION PROCESS

Recently, more focus has been put on the use of silicon as bulk material in MEMS. Using silicon as structure, we can get many benefits which are well defined mechanical properties, low intrinsic stress, endurance, high Young's modulus and electrical characteristics.

The goal of the present study is fabrications of high resolution accelerometer using simple process. To archive this goal, the structure have proper height to get large proof mass and large sensing area, and only 3 masks are used in full process.

The key point of this fabrication is eutectic bonding. The glass wafer makes electrical isolation between proof mass and substrate. Anchor and gold electrode is pre-defined on the silicon and glass wafer respectively, and bonded together by eutectic bonding. However, it is hard to make electrical open/short state using bonding process. Therefore, we used Au layer for not only an adhesion layer but also an electrode layer, and the stiction problem due to wet release process can be removed by this process at the same time.

3.1 Detail

Figure 6 shows the fabrication process flow of the designed acceleration sensor.

Glass wafer is Pyrex7740 whose thermal expansion coefficient is similar to silicon. Glass wafer is coated with 1000Å thick Au layer using metal sputter, and then patterned. The role of Au layer is electrode as well as intermediate layer for eutectic bonding.

Next, two wafers are precisely align bonded together using eutectic bonding. Anchor pattern should be bonded strongly on the Au electrode pattern. This step removes wet environmental release process which causes stiction.

Backside of silicon wafer is patterned by Deep RIE to 10um deep using PR mask. This pattern is an anchor which standing on glass wafer.

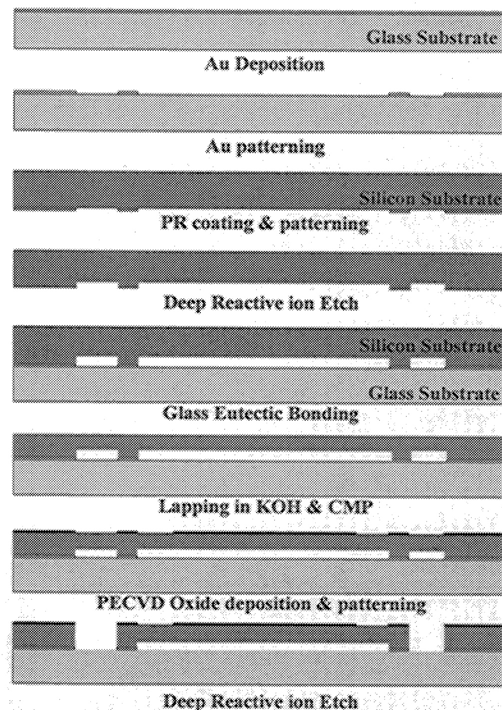

Figure 6 : Fabrication Process

Silicon side of bonded wafer is etched in KOH to get desired structure height roughly(about 60um). On account of the high roughness of etched silicon surface, chemical mechanical polishing(CMP) process should be performed. Also, CMP process makes silicon structure height to 50um. After CMP process, metal slurry exists on silicon surface. To remove this residue, post-CMP process is necessary.

On the silicon surface, PECVD silicon dioxide which is used as etch mask is deposited to 3000Å and patterned by RIE. Final step is structure pattern definition, and silicon etched to the bottom using Deep RIE.

4 CAPACITANCE MEASUREMENT

Capacitive sensor measures capacitance change which induced by displacement of moving mass. There are many types of measurement scheme such as charge integration, op-amp buffer, and JFET buffer. Among these scheme, we adopted charge integration method. Figure 7 is schematic view of charge integration method. Charge amplifier integrates the charge which is induced in proof mass. Output signal is very sensitive to displacement, and almost not influenced by parasitic capacitance. The output signal is delivered to filter and amplifier for signal conditioning.

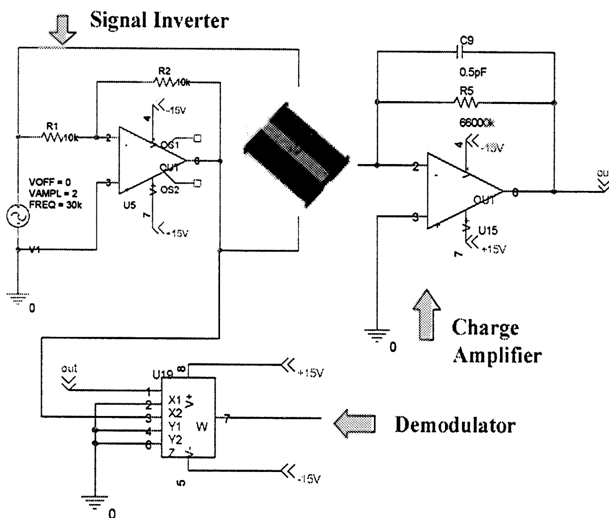

Figure 7 : Interface Circuit

5 CONCLUSION

High precision differential capacitive accelerometer was designed and have been fabricated. At the same time, interface circuit is designed and made.

The present accelerometer has high aspect ratio structure, therefore high resolution and insensitivity to noise can be achieved. Fabrications of the accelerometer is distinguished from other silicon glass bonded type by special bonding technique. This bonding process allows stiction-free process too. The similar fabrication process can be applied to gyroscope.

REFERENCES

[1] O. Ludtke, V. Biefeld, A. Buhrdorf, J. Binder "Laterally driven accelerometer fabricated in single crystal silicon" Sensors & Actuators, pp. 149-154, 2000.

[2] Jason W. Weigold, khalil Najafi, Stella W. Pang "Design and fabrication of Submicrometer, Single crystal Si accelerometer" IEEE Journal of MEMS Vol.10, No. 4, pp 518-524, 2001.

[3] T.B. Gabrielson "Mechanical-Thermal nosie in micromachined acoustic and vibration sensors" IEEE Trans, Electron Device, vol 40, pp. 903-909, 1993.

[4] J. Chae, H. Kulah, and K. Najafi, "A Hybrid Silicon-On-Glass (SOG) Lateral Micro-Accelerometer with CMOS Readout Circuitry," MEMS'02, pp. 623-626, Las Vegas, January 2002

[5] K.Y. Park, C.W. Lee, H.S. Jang, Y.S. Oh, "Capacitive type surface micromachined silicon accelerometer with stiffness tuning capability." Sensors & Actuators, pp. 109-116, 1999.

[6] B. E. Boser and R. T. Howe, "Surface Micromachined Accelerometers", IEEE J. Solid-State Circuits, vol. SC-31, pp. 366–375, March 1996.

[7] M. A. Lemkin and B. E. Boser, "A Micromachined Fully Differential Lateral Accelerometer", in CICC Dig. Tech. Papers, pp. 315–318, May 1996.

[8] Francis E. H. Tay, J. Xu, V. J. Logeeswaran "A differential capacitive low-g micro accelerometer with mg resolution" Sensors & Actuators, pp. 45-51, 2001.

[9] Wenmin Qu, Christian Wenzel, Gerald Gerlach "Fabrication of a 3D differential -capacitive acceleration sensor by UV-LIGA." Sensors & Actuators, pp. 14-20, 1999.

[10] James B. Starr "Squeeze Film Damping in Solid State Accelerometers." Technical Digest IEEE Solid State Sensor and Actuator Workshop, pp 44-47, June 1990.